#### Journal of Physics: Conference Series

#### **PAPER • OPEN ACCESS**

# Analysis of Deterioration in a Plasma Focus Device

To cite this article: Daniel Zanelli et al 2018 J. Phys.: Conf. Ser. 1043 012049

View the article online for updates and enhancements.

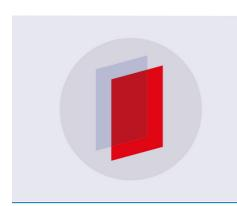
#### Related content

Ghazi

- A Method to Obtain Higher Current Density in the Plasma Focus Masato Itoh, Kenichi Hatori and Katsumi Hirano
- Morphological and structural effects on tungsten targets produced by fusion plasma pulses from a table top plasma focus

M.J. Inestrosa-Izurieta, E. Ramos-Moore and L. Soto

 Reliability analysis on a shell and tube heat exchanger
 S Lingeswara, R Omar and T I Mohd



## IOP ebooks™

Bringing you innovative digital publishing with leading voices to create your essential collection of books in STEM research

Start exploring the collection - download the first chapter of every title for free.

### Analysis of Deterioration in a Plasma Focus Device

Daniel Zanelli<sup>1,\*</sup>, Enrique López<sup>1</sup>, Cristian Pavez<sup>2,3,4</sup>, José Pedreros<sup>3</sup>, Jalaj Jain<sup>3,5</sup>, Gonzalo Avaria<sup>2,3,4</sup>, José Moreno<sup>2,3,4</sup>, Biswajit Bora<sup>2,3,4</sup>, Sergio Davis<sup>2,3,4</sup> and Leopoldo Soto<sup>2,3,4,\*</sup>

- 1 Facultad de Ciencias Físicas y Matemáticas, Universidad de Chile
- 2 Comisión Chilena de Energía Nuclear, Casilla 188-D, Santiago Chile
- 3 Center for Research and Applications in Plasma Physics and Pulsed Power P4, Chile
- 4 Universidad Andres Bello, Departamento de Ciencias Físicas, República 220, Santiago, Chile
- 5 Universidad de Talca, Chile
- \* email: zanelli.93@gmail.com, lsoto@cchen.cl

Abstract. The Plasma Focus (PF) is a kind of dense transient plasmas in with high-pulsed voltage. To produce devices for eld application it is necessary to obtain PF equipment able to operate for a long period of time. Thus, a reliability analysis is indispensable. In this work a reliability analysis program for plasma focus devices is presented. The program considers a criticality analysis using Failure Modes and Effects Criticality Analysis (FMECA) to identify the most important failure modes of the system. Said failure modes are studied operating the Plasma Focus for many cycles, obtaining from them the characteristic curves of V(t) and  $\dot{I}(t)$ . Feature Extraction (FE) techniques are applied to obtain a list of parameters that correlate to the degrading process. Furthermore, Machine Learning tools are used to learn from the obtained data, linking the changes in these parameters during its life cycle to the decay of the system in hope for future implementation of a predictive maintenance system and a reference for data analysis and prediction in PFs. The study was applied to a portable plasma focus device operated at 2 joules of stored energy.

#### 1. Introduction

In plasma focus (PF) devices high voltage is applied to a low pressure gas between coaxial cylindrical electrodes separated by an insulator. Due to its capacity to produce hot/warm and dense plasmas [1, 2]; intense beams of charged particles, neutrons [3-5], x-ray emission [6-8], plasma shocks [9], filaments [10] and jets are generated [11]. Thus, it has become a laboratory for fundamental and applied research related to fusion, neutron production [3-5], hard x-ray [6-8], high brightness soft x-ray production, material for fusion reactors [9, 12], astrophysical phenomena [10, 11] and biology [13]. Also, the PF has attracted the attention of the plasma research community as non-radioactive radiation source for industrial and field applications. In particular, at the Chilean Nuclear Energy Commission (CCHEN) the scale rules to develop miniaturized plasma focus devices has been determined [14]. In the last year several table top and portable plasma focus devices have been designed and constructed at CCHEN [3-5, 15]. In this study a deterioration model of the system as the life cycle progresses is developed. In which, a Failure Modes and Eects Criticality Analysis (FMECA) is done to a small tabletop plasma focus operating at few joules (PF-2J). Following an analysis of the characteristic electrical signals of plasma focus devices is implemented to correlate an advance in its wear. This is done in the

Content from this work may be used under the terms of the Creative Commons Attribution 3.0 licence. Any further distribution of this work must maintain attribution to the author(s) and the title of the work, journal citation and DOI.



Figure 1. Photograph of PF-2J

most critical failure mode using Feature Extraction techniques to compare a linear model and a nonlinear Neural Network (NN) model.

#### 1.1. The PF-2J Device

A portable plasma focus operating at few joules for field applications was designed and constructed at CCHEN. The device, PF-2J, including the capacitor, spark-gap, discharge chamber and power supply is portable in a hand luggage with a total weight of less than 1.5kg. The capacitor has 120nF. The measured total external inductance is 40nH. The total impedance of the generator is in the order of  $0.58\Omega$ . The device operates from 6 to 8kV charging voltage (i.e.  $\sim 2-4J$ ), achieving 9 to 13kA in 120ns. Figure 1 shows a photograph of the PF-2J.

#### 2. Failure Modes and Effects Criticality Analysis

When performing the analysis, a series of key elements were considered, with their respective failure modes: the severity that this failure mode entails, the detectability of the failure and its probability of occurrence.

Each of these elements are assigned a value between 0 and 10 to describe the failure mode. Later a criticality factor is determined by the multiplication of these values. The results of this preliminary analysis is shown in table 1.

From this table a tendency of certain failure modes to be much more critical than others can clearly be seen. Specifically for the Insulator, the deposition of a conductive film around it has become the most critical failure mode, as well as the most frequent cause of failure for most PF equipments.

This is why this study will be focused on the detection of wear associated to the thin layer of material that degrades the insulator from its dielectric properties.

Table 1.	FMECA	Results	tor	PF-2	<u>′J</u>
Failu	re Mode	S	$\mid \mathbf{S} \mid$	ev.	P

Elements	Failure Modes	Sev.	Prob.	Det.	Criticality
Capacitor	Burning	6	5	4	120
	Short Circuit	5	6	5	150
Spark Gap	Corrosion Electrodes	5	3	4	60
Anode	Corrosion	5	3	3	45
Insulator	Deposition of Conductive Film	6	7	5	210
Cathodes	Corrosion	5	3	3	45
Discharge Chamber	Gas Filtrations	3	4	5	60
Spark Gap Chamber	Gas Filtrations	3	4	5	60
Gas Connectors	Gas Filtrations	3	4	5	60
Viewers	Reduced Visibility	2	3	1	6
	Breaking	4	1	1	4
Electrical Connectors	Burning	6	5	3	90
	Short Circuit	5	5	3	75
Measurers	External Failure	2	4	5	40
Power Supply	Burning	5	2	5	50
Vacuum Pump	External Failure	2	2	5	20
Gas Tank	External Failure	2	2	3	12

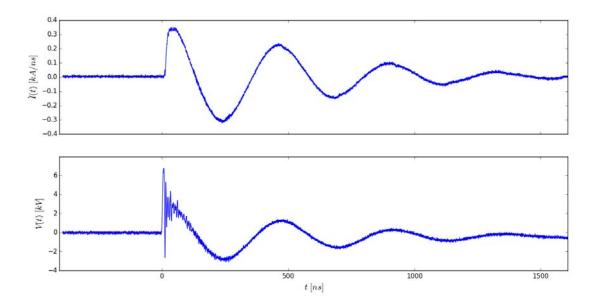
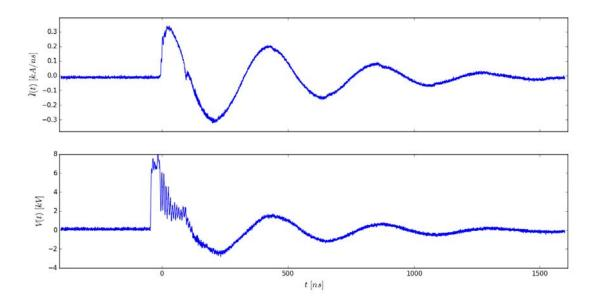


Figure 2. Caracteristic Signals of PF-2J in a shot with absence of z-pinch

#### 3. Caracteristic Signals and Feature Extraction

The characteristic electrical signals of the PF-2J are shown in figure 2 without dense plasma pinching and in figure 3 with pinching 95ns after the discharge. It should be noted that these curves correspond to a damped harmonic oscillation coming from the RLC circuit that is formed in the equipment. The following characteristic signals were generated by charging the PF-2J at 6kV with  $H_2$  gas filled in the discharge chamber at 8mbar.



**Figure 3.** Caracteristic Signals of PF-2J in a shot with z-pinch at 95[ns]

For this reason, another program has been developed in python that analyzes the signals and extracts parameters that describe it in several ways. Here comes the Feature Extraction concept, as it is presented in [16], where signal data analysis is performed. In this case, the chosen features are described in equations 1 to 4, where  $n_j$  is the j element of the function, u is the mean,  $\sigma$  is the standard deviation and N is the number of elements in the function.

$$Kurtosis = \frac{\sum_{j=1}^{N} (n_j - u)^4}{(N-1)\sigma^4}$$
 (1)

Clearance Indicator = 
$$\frac{max|n|}{\sqrt{\frac{1}{N}\sum_{j=1}^{N}(n_j)^2}}$$
 (2)

$$Clearance\ Indicator = \frac{max|n|}{\sqrt{\frac{1}{N}\sum_{j=1}^{N}(n_j)^2}}$$

$$Shape\ Indicator = \frac{\sqrt{\frac{1}{N}\sum_{j=1}^{N}(n_j)^2}}{\frac{1}{N}\sum_{j=1}^{N}|n_j|}$$

$$ClearanceIndicator = \frac{max|n|}{(\frac{1}{N}\sum_{j=1}^{N}\sqrt{|n_j|})^2}$$

$$(3)$$

$$ClearanceIndicator = \frac{max|n|}{(\frac{1}{N}\sum_{j=1}^{N}\sqrt{|n_j|})^2}$$
(4)

The results of the evolution of the mentioned features as a function of the number of discharges are shown below. In the figure 4 the values of Kurtosis, Crest Indicator, Clearance Indicator and Shape Indicator for I(t) are shown, in the figure 5 the same features for the V(t) signal are

Considering that the experiment presented instances of Pinch from the vicinity of N = 1000, this moment (after 1000 discharges) is considered as the reference point of the beginning of the degradation, since the values before this correspond to the conditioning of the insulator prior to the life cycle. Taking this into account, it is convenient to find the proportional change to the reference point, where F is a feature of the system, the percentage change is defined as in the equation 5.

IOP Conf. Series: Journal of Physics: Conf. Series 1043 (2018) 012049

doi:10.1088/1742-6596/1043/1/012049

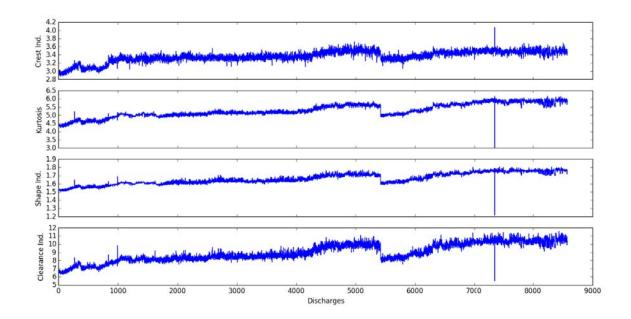


Figure 4. Feature Extraction of  $\dot{I}(t)$ 

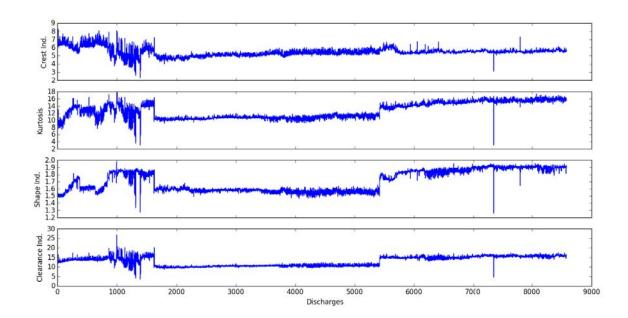


Figure 5. Feature Extraction of V(t)

$$\Delta F_x = \frac{F(N_x) - F(N = 1000)}{F(N = 1000)} \times 100 \tag{5}$$

#### 4. Degradation Models

According to the data that arise from the experiment, relationships can be established between the evolutions of the different characteristic features over time with the advance in the life cycle of the equipment.

To approach the model that allows to correlate these states, an analytical relationship can be established between a multidimensional space, the features, towards a one-dimensional space, the wear and tear. Hence it can be denoted  $\overrightarrow{F}$  to the vector that contains all features after normalization. It is crucial to normalize the features to a point of reference so that the model can be applied to multiple experiments.

If a relationship exists between the change in features and the wear of the equipment, it can be assumed that there is a function Y such that:

$$Y(\cdot): \Re^n \to \Re \mid Y(\overrightarrow{F}) = N \tag{6}$$

Where N is the amount of discharges that the insulator of the equipment has endured until an arbitrary time.

#### 4.1. Estimating N With a Linear Combination

The first approach to estimate this function could be to opt for linear behavior. Although there is a loss of information given by the approximation of the curves 4 and 5 to a linear behavior, the fact that the phenomenon is seen in several dimensions allows for eliminating sources of noise, while maintaining a simple and direct approach.

For this, the noise of the curves  $F_i(N)$  is reduced by using the Signal library of python using the function signal.lfilter() and then a linear interpolation in order to obtain an analytical resolution for the estimation of N, for each of the  $F_i$ . That is to say:

$$\overrightarrow{N}_{estimated} = \begin{bmatrix} N_1 \\ N_2 \\ N_3 \\ \vdots \\ N_n \end{bmatrix} = \begin{bmatrix} y_1(F_n) \\ y_2(F_n) \\ y_3(F_n) \\ \vdots \\ y_n(F_n) \end{bmatrix}$$

$$(7)$$

Where  $y_i = m_i \ cdot F_i + n_i$  represents the equation of the interpolated line for the inverse graphs of  $F_i(N)$ .

This way, a linear estimation of the number of discharges made for each parameter can be obtained. However, now there are many estimates for the same result. Considering that it is possible to make a global estimate of N as a linear combination of the estimates for each feature:

$$N_{est} = C_1 \cdot N_1^{est} + C_2 \cdot N_2^{est} + C_3 \cdot N_3^{est} + \dots + C_n \cdot N_n^{est}$$

$$N_{est} = \sum_{i} C_i \cdot N_i^{est}$$
(8)

In this equation all the  $N_i^{est}$  are known for each of the n features and N discharges, so the coefficients that best represent reality can be found, contrasting them with the real number of shots corresponding to the feature vector. To find the coefficients  $C_i$  of each of these features, a crucial problem occurs in the change of dimensionality, because n corresponds to the total number of features and N to the total number of discharges, there are  $n \sim 10$  variables and  $N \simeq 8000$  equations. So it is proposed to solve the problem as if there were just n equations, being these the first n, then solving it again with the equations n to 2n, and so on until solving all the N equations using N/n linear combinations:

$$1 = C_{1} \cdot N_{1}^{est}(1) + C_{2} \cdot N_{2}^{est}(1) + \dots + C_{n} \cdot N_{n}^{est}(1)$$

$$2 = C_{1} \cdot N_{1}^{est}(2) + C_{2} \cdot N_{2}^{est}(2) + \dots + C_{n} \cdot N_{n}^{est}(2)$$

$$3 = C_{1} \cdot N_{1}^{est}(3) + C_{2} \cdot N_{2}^{est}(3) + \dots + C_{n} \cdot N_{n}^{est}(3)$$

$$\dots$$

$$n = C_{1} \cdot N_{1}^{est}(n) + C_{2} \cdot N_{2}^{est}(n) + \dots + C_{n} \cdot N_{n}^{est}(n)$$

$$(9)$$

And the same for the next n equations:

$$n+1 = C_1 \cdot N_1^{est}(n+1) + C_2 \cdot N_2^{est}(n+1) + \dots + C_n \cdot N_n^{est}(n+1)$$

$$n+2 = C_1 \cdot N_1^{est}(n+2) + C_2 \cdot N_2^{est}(n+2) + \dots + C_n \cdot N_n^{est}(n+2)$$

$$n+3 = C_1 \cdot N_1^{est}(n+3) + C_2 \cdot N_2^{est}(n+3) + \dots + C_n \cdot N_n^{est}(n+3)$$
...
$$2n = C_1 \cdot N_1^{est}(2n) + C_2 \cdot N_2^{est}(2n) + \dots + C_n \cdot N_n^{est}(2n)$$
(10)

This way N/n linear systems can be solved to obtain the n coefficients  $C_i$ , N/n times. These systems can be expressed in a matrix form for simplicity:

$$\begin{bmatrix} 1 \\ 2 \\ 3 \\ \vdots \\ n \end{bmatrix} = \begin{bmatrix} N_1^{est}(1) & N_2^{est}(1) & \dots & N_n^{est}(1) \\ N_1^{est}(2) & N_2^{est}(2) & \dots & N_n^{est}(2) \\ N_1^{est}(3) & N_2^{est}(3) & \dots & N_n^{est}(3) \\ \vdots \\ N_1^{est}(n) & N_2^{est}(n) & \dots & N_n^{est}(n) \end{bmatrix} \cdot \begin{bmatrix} C_1 \\ C_2 \\ C_3 \\ \vdots \\ C_n \end{bmatrix}$$

$$(11)$$

$$\overrightarrow{N}_{real} = \overrightarrow{N}_{est} \cdot \overrightarrow{C}$$

This way the number of discharges made by the equipments can be estimated through a linear combination of features.

$$N_{est} = \sum_{i} C_i \cdot F_i \tag{13}$$

Using the experimental data, the predictions of  $N_{est}$  can be found by solving the linear system for the features presented in 4 and 5, obtaining an estimate of N for each set of features as shown in figure 6.

#### 4.2. Estimating N With a Neural Network

Considering that a linear analysis is simple, fast and of good results, it is an analysis that can be too basic for such a complex problem. We are not only extrapolating the data getting away from the real spectrum once, but twice, thanks to the estimates of  $N_i^{est}$  and  $C_i$ .

Which is why a model of neural networks is proposed. It allows to iteratively relate the collected data, in order to approximate the ideal function  $Y(\overrightarrow{F})$ . In this study a neural network of 4 layers is used, 2 visible and 2 hidden, as shown in the figure 7.

The weights of the neural network are the state variables of the system, they describe the function  $Y(\overrightarrow{F})$ . These are contained in matrices  $W_0$ ,  $W_1$  and  $W_2$ , which determine the status of the network's computation after prolonged training.

IOP Conf. Series: Journal of Physics: Conf. Series 1043 (2018) 012049

doi:10.1088/1742-6596/1043/1/012049

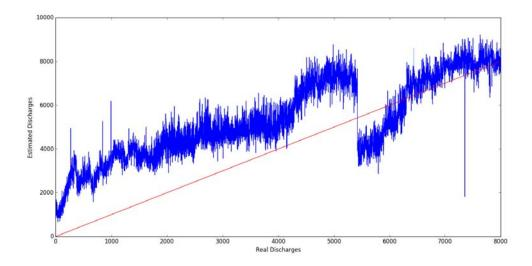


**Figure 6.** Estimates of N with Linear Combination. Note that the discontinuity at  $N \approx 5500$  present in all features (figures 4 and 5) is due to the disassembly of the spark-gap, nevertheless it returns to the trend.

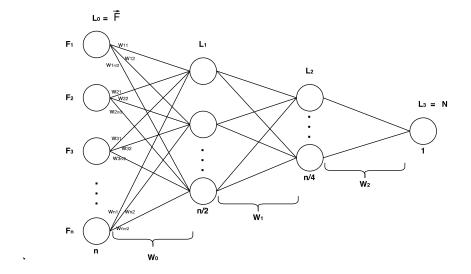


Figure 7. Diagram of Neural Network Used

For simplicity, the number of nodes in layers 1 and 2 was chosen as half of nodes in the previous layer, thus ensuring a smooth transition in dimensional reduction. Therefore the dimensions of the matrices  $W_0$ ,  $W_1$  y  $W_2$  are  $(n \times \frac{n}{2})$ ,  $(\frac{n}{2} \times \frac{n}{4})$  and  $(\frac{n}{4} \times 1)$ , respectively.

This neural network consists of a basic Perceptron of two hidden layers, where each neuron of the hidden layers acts according to the sigmoid function of the linear combination of each  $F_i$  weighted by each of its  $w_{ji}$ . Meaning that each node i in any layer has a value given by the previous layer, as described in equations 14-16.

IOP Conf. Series: Journal of Physics: Conf. Series 1043 (2018) 012049 d

doi:10.1088/1742-6596/1043/1/012049

$$L_1[i] = \sigma\left(\sum_j w_{ji} \cdot L_0[j]\right) = \sigma\left(\sum_j w_{ji} \cdot F_j\right)$$
(14)

$$L_2[i] = \sigma\left(\sum_{j} w'_{ji} \cdot L_1[j]\right) \tag{15}$$

$$N = L_3 = \sigma \left( \sum_j w_j'' \cdot L_2[j] \right) \tag{16}$$

With the sigmoid function defined as:

$$\sigma(x) = \frac{1}{1 + e^{-x}} \tag{17}$$

The neural networks initially operate using matrices of weights generated at random, then the error is calculated according to the prediction made in contrast to the actual value provided by the training data. This error is propagated from the last layer to each of the nodes, allowing to know what the impact of each weight to the final error using the *backpropagation* technique. This technique along with many neural network operations are extensively detailed in [17].

With this neural network an analysis can be made to the data to obtain an estimate of N, as in the linear combination analysis. Using the same parameters studied in the previous model, the neural network is trained by associating the series of features with a value of N.

It should be noted that the data was delivered to the neural network in a random order, without losing the correspondence between a series of values  $\overrightarrow{F}$  and the N associated to each. This ensures that learning is not distorted by the chronological order of the data, resulting in the graph shown in figure 8

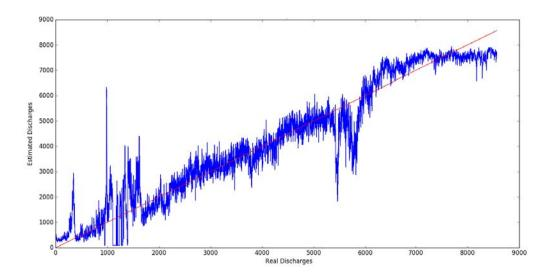


**Figure 8.** Estimates of N With Neural Networks. Note that the discontinuity at  $N \approx 5500$  is much less severe using this method than with lineal combination

#### 5. Conclusion

From this analysis it can be said that by observing the characteristic signals emitted during a regular discharge of a PF equipment, certain descriptive features can be obtained and aid in determining the current state of the equipment.

Furthermore, it can be concluded that rough predictions can be made about the discharges made by observing certain key parameters. In particular, Kurtosis, Shape Indicator, Clearance Indicator and Crest Indicator of the characteristic signals V(t) and  $\dot{I}(t)$ . Furthermore the actual state of degradation of the PF equipment can be estimated through linear combination and neural network approaches.

Considering that the shape indicator, clearance indicator, kurtosis and crest indicator increase as the experiment evolves, this can be characterized as one phenomenon: the damping of the oscillation is greater. This explains the evolution of these parameters simultaneously. On the other hand, it is a good option to rely on a range of parameters that make evidence of the same phenomenon since they ensure that it is a global trend and not a corruption of the data.

In such a problem it can be seen from the figures 6 and 8 that a nonlinear neural network approach is much more suitable for determining a function that reduces the dimensionality spectrum, as is  $Y(\overrightarrow{F})$ .

Describing the overall performance and deterioration is crucial to arrive at better designs and best practices in plasma focus devices. Although this represents an initial model for understanding the degradation of the PF-2J, future research is important to understand the wear phenomenon in plasma focus devices and similar equipment.

#### Acknowledgement

The work is supported by IAEA CRP contract 20370 and by grant ACT-1115, CONICYT, Chile.

#### References

- [1] Leopoldo Soto, Plasma Physics and Controlled Fusion 47, A361 (2005) New Trends and Future Perspectives on Plasma Focus Research
- [2] Ariel Tarifeño, Cristian Pavez, José Moreno and Leopoldo Soto, IEEE Trans. Plasma Science, 39, 756 (2011)

  Dynamics and Density Measurements in a Small Plasma Focus of Tens of Joules Emitting Neutrons
- [3] P. Silva, J. Moreno, L. Soto, L. Birstein, R. Mayer, W. Kies, Applied Physics Letters 83, 3269 (2003) Neutron Emission from a Fast Plasma Focus of 400 Joules
- [4] Leopoldo Soto, Patricio Silva, José Moreno Moreno, Marcelo Zambra, Walter Kies, Roberto E. Mayer, Alejandro Clausse, Luis Altamirano, Cristian Pavez, and Luis Huerta J. Phys. D: App. Phys. 41, 205215 (2008). Demonstration of neutron production in a table top pinch plasma focus device operated at only tens of joules.
- [5] Leopoldo Soto, Cristian Pavéz, José Moreno, Luis Altamirano, Luis Huerta, Mario Barbaglia, Alejandro Clausse, and Roberto E. Mayer, Physics of Plasmas 24, 082703 (2017) Evidence of nuclear fusion neutrons in an extremely small plasma focus device operating at 0.1 Joules
- [6] Mario Barbaglia, Horacio Bruzzone, H. Acuña, Leopoldo Soto and Alejandro Clausse, Plasma Physics and Controlled Fusion 51, 045001 (2009) Experimental study of the hard x-ray emissions in a Plasma Focus of hundreds of Joules
- [7] Cristian Pavez and Leopoldo Soto, IEEE Trans. Plasma Science, 38, 1132 (2010) Demonstration of x-ray Emission from an ultraminiature pinch plasma focus discharge operating at 0.1 J. Nanofocus
- [8] C Pavez, M Zambra, F Veloso, J Moreno and L Soto, Journal of Physics: Conference Series 511, 012028 (2014) Potentiality of a table top plasma focus as X-ray source: Radiographic applications
- [9] L. Soto, C. Pavez, J. Moreno, M. J. Inestrosa-Izurieta, F. Veloso, G. Gutiérrez, J. Vergara, A. Clausse, H. Bruzzone, F. Castillo, and L. F. Delgado-Aparicio, Physics of Plasma 21, 122703 (2014) Characterization of the axial plasma shock in a table top plasma focus after the pinch and its possible application to testing materials for fusion reactors

- [10] Leopoldo Soto, Cristian Pavez, Fermin Castillo, Felipe Veloso, José Moreno, and S. K. H. Auluck, Physics of Plasmas 21, 072702 (2014) Filamentary structures in dense plasma focus: current filaments or vortex filaments
- [11] C. Pavez, J. Pedreros, A. Tarifeño Saldivia and L. Soto, Physics of Plasmas 22, 040705 (2015) Observations of plasma jets in a table top plasma focus discharge
- [12] M.J. Inestrosa-Izurieta, E. Ramos-Moore and L. Soto, Nuclear Fusion 55, 093011 (2015) Morphological and structural effects on tungsten targets produced by fusion plasma pulses from a table top plasma focus
- [13] J. Jain, J. Moreno, R. Andaur, R. Armisen, D. Morales, K. Marcelain, G. Avaria, B. Bora, S. Davis, C. Pavez, and L. Soto, AIP Advances 7, 085121 (2017) Hundred joules plasma focus device as a potential pulsed source for in vitro cancer cell irradiation
- [14] Leopoldo Soto, Cristian Pavez, Ariel Tarifeño, José Moreno and Felipe Veloso, Plasma Sources Sci. and Technol. 19, 055017 (2010) Studies on scalability and scaling laws for the plasma focus: similarities and differences in devices from 1MJ to 0.1J
- [15] L. Soto, C. Pavez, J. Moreno, J. Pedreros and L. Altamirano, Journal of Physics: Conference Series 511, 012032 (2014) Non-radioactive Source for Field Applications Based in a Plasma Focus of 2J: Pinch evidence
- [16] Kwok L. Tsui, Nan Chen, Qiang Zhou, Yizhen Hai, Wenbin Wang. 2015. Mathematical Problems in Engineering Volume 2015, Article ID 7931612015. Prognostics and Health Management: A Review on Data Driven Approaches
- [17] Ryszard Tadeusiewcz. 1992 Sieci Neuronowe, Akademicka Oficyna Wydawnicza